

# UC San Diego

## UC San Diego Previously Published Works

### Title

The long non-coding RNA MALAT1 regulates intestine host-microbe interactions and polyposis

### Permalink

<https://escholarship.org/uc/item/4qp2t942>

### Authors

Long, Tianyun  
Hernandez, Juan E  
Ma, Shengyun  
[et al.](#)

### Publication Date

2023

### DOI

10.3389/fcell.2023.1168693

### Copyright Information

This work is made available under the terms of a Creative Commons Attribution License, available at <https://creativecommons.org/licenses/by/4.0/>

Peer reviewed

**The long non-coding RNA MALAT1 regulates  
intestine host-microbe interactions and polyposis**

Tianyun Long<sup>1</sup>, Juan E. Hernandez<sup>1</sup>, Shengyun Ma<sup>1</sup>, Scarlet Steele<sup>1</sup>, Claire Luo<sup>1</sup>, Yuxin Li<sup>1</sup>,  
Qinghong Xie<sup>1</sup>, Francesca Telese<sup>2</sup>, Bing Zhou<sup>3,4</sup>, Wendy Jia Men Huang<sup>1, \*</sup>

<sup>1</sup> Department of Cellular and Molecular Medicine, University of California San Diego, La Jolla, CA,  
USA

<sup>2</sup> Department of Psychiatry, University of California San Diego, La Jolla, CA, USA

<sup>3</sup> State Key Laboratory of Stem Cell and Reproductive Biology, Institute of Zoology Chinese  
Academy of Sciences, Beijing, China

<sup>4</sup> Beijing Institute for Stem Cell and Regenerative Medicine, Beijing, China

\* Correspondence: [wendyjmh Huang@health.ucsd.edu](mailto:wendyjmh Huang@health.ucsd.edu)

## **Abstract**

The long non-coding RNA (lncRNA) Metastasis-associated lung adenocarcinoma transcript 1 (MALAT1) maintains the integrity of the intestinal epithelial barrier and regulates local inflammation. However, its influences on intestinal microbial communities and tissue susceptibility to cancer development remain unexplored. Here, we report that MALAT1 regulates host anti-microbial response gene expression and the composition of mucosal-associated microbial communities in a region-specific manner. In the APC mutant mouse model of intestine tumorigenesis, knocking out MALAT1 results in higher polyp counts in the small intestine and colon. Interestingly, intestine polyps that developed in the absence of MALAT1 were smaller in size. These findings highlight the unexpected bivalent role of MALAT1 in restricting and promoting cancer progression at different disease stages. Among the 30 MALAT1-targets shared by both the small intestine and colon, ZNF638 and SENP8 levels are predictive of colon adenoma patient overall survival and disease-free survival. Genomic assays further revealed that MALAT1 modulates intestinal target expression and splicing through both direct and indirect mechanisms. This study expands the role of lncRNAs in regulating intestine homeostasis, microbial communities, and cancer pathogenesis.

## Introduction

Intestinal epithelial cells (IECs) provide a physical barrier against microbes and facilitate local immune responses<sup>1</sup>. Genetic mutations and microbial challenges that impair IEC functions contribute to gastrointestinal illnesses like inflammatory bowel disease and colorectal cancer<sup>2-5</sup>. However, our understanding of the molecular regulators of IECs remains incomplete. The evolutionarily conserved Metastasis-associated lung adenocarcinoma transcript 1 (MALAT1), also known as nuclear enrichment autosomal transcript 2 (NEAT2), is one of the most abundantly expressed long non-coding RNAs (lncRNAs) in IECs. Recent studies suggest that human MALAT1 has an important role in maintaining the integrity of the intestinal epithelial barrier and contributes to local inflammation. By sequestering target microRNAs, MALAT1 maintains the expression of apical junction complex proteins NUMB and CLDN11<sup>6</sup>. In Crohn's disease patients and the dextran sulfate sodium-induced mouse model of colitis, MALAT1 is downregulated<sup>6</sup>. In Ulcerative colitis patients, however, MALAT1 is upregulated<sup>2</sup>. However, the physiologic and pathologic functions of MALAT1 in the intestine epithelium under homeostasis and disease settings remain unclear.

Mechanistic studies on MALAT1 have been performed in the context of lung, breast, cervix, and esophageal cancers, where MALAT1 expression is often dysregulated<sup>4,7-10</sup>. Cell culture studies suggest that MALAT1 is enriched in the nucleus and regulates gene expression at multiple levels<sup>11-17</sup>. For example, it can interact with transcription factors and chromatin remodelers such as PRC2 to regulate transcription, pre-mRNA splicing, and act as a sponge to sequester microRNAs<sup>8,18-25</sup>. Yet, the extent to which these mechanisms contribute to MALAT1 function *in vivo* under homeostasis and disease settings remains unclear.

In this study, we report that murine MALAT1 regulates the transcription and alternative splicing of a subset of IEC genes involved in microbial responses through both direct chromatin recruitment and indirect mechanisms. Knocking out MALAT1 results in altered intestine microbial

communities and increases susceptibility to developing polyps in the small intestine and colon. These findings highlight the unexpected tumor suppressor function of MALAT1 in intestine tumorigenesis and provide insights into the contributions of lncRNAs in regulating IEC functions and the discovery of new therapeutic targets for intestinal cancers.

## Results

### MALAT1 regulates the abundance and splicing of IEC genes involved in anti-microbial responses.

MALAT1 is one of the most highly expressed long non-coding RNAs in both the small intestine and colon epithelium (Fig. 1A). Previous studies suggest that MALAT1 can regulate gene expression at the transcriptional and post-transcriptional levels<sup>19,20</sup>. Based on these reports, we hypothesized that MALAT1 may contribute to intestine functions by regulating gene expressions in intestine epithelial cells. To test this possibility, we crossed the *Malat1*<sup>+/-</sup> mice to generate gender-matched and cohoused control (CTL, *Malat1*<sup>+/+</sup> and *Malat1*<sup>+/-</sup>) and *Malat1* knockout (*Malat1*<sup>-/-</sup>) littermates for our study. CTL and *Malat1*<sup>-/-</sup> littermates were born in Mendelian ratios and all survive to adulthood without notable spontaneous diseases, which is consistent with a previous report<sup>26</sup>. CTL and *Malat1*<sup>-/-</sup> littermates showed similar weights for the duration of our experiments between days 50 and 130 (Fig. 1B). H&E staining of the CTL and *Malat1*<sup>-/-</sup> colonic sections confirmed similar intestine epithelium morphology (Fig. 1C-D). To assess intestine barrier function, mice were orally gavaged with 4kDa Fluorescein isothiocyanate-dextran (FITC-dextran) together with 70kDa Rhodamine B isothiocyanate-dextran (RITC-dextran). In the CTL and *Malat1*<sup>-/-</sup> bloodstream, we found similar levels of RITC-dextran, indicating *Malat1*<sup>-/-</sup> mice have intact barrier activity against bacteria-size macromolecules. Interestingly, *Malat1*<sup>-/-</sup> mice showed reduced levels of serum FITC-dextran, suggesting that MALAT1 promotes protein-size macromolecule passage in the intestine (Fig. 1E).

To elucidate the mechanism(s) underlying MALAT1 function in the intestine, we isolated small intestine and colon IECs from two pairs of 8-week-old wildtype and MALAT1 knockout female cohoused littermates for differential transcriptome and splicing analyses. Differential gene expression analysis identified 67 and 143 MALAT1-dependent small intestine and colon IEC transcripts, respectively (Fig. 2A, Table S1). Splicing analysis was performed using rMATS<sup>27</sup> and revealed a larger MALAT1-regulatory footprint (Fig. 2B, Table S2 and S3). The majority of the MALAT1-dependent alternative splicing events in both small intestine and colon are skipped exons. These results indicate MALAT1 regulates RNA abundance and processing in both the small intestine and colon and that its higher expression levels in the colonic epithelium are associated with a larger set of MALAT1-dependent targets identified in that tissue. We selected two genes that displayed MALAT1-dependent splicing patterns for validation by flow cytometry and confirmed a reduced proportion of TGF- $\beta$  receptor 1-positive IECs in the *Malat1*<sup>-/-</sup> small intestine (Supplementary Fig. S1A-B) and an increased proportion of IL-27 receptor alpha-positive IECs in the *Malat1*<sup>-/-</sup> colon (Supplementary Fig. S1C-D).

Gene Ontology analysis of the IEC genes relying on MALAT1 at the expression and/or splicing levels revealed enrichment for pathways implicated in anti-microbial responses in both the small intestine and colon (Fig. 3A and Supplementary Fig. S2A). Therefore, we performed meta-genomic analysis to test whether alterations in anti-microbial response programs in the *Malat1*-deficient epithelium may be associated with changes to the mucosal-associated microbial communities. Interestingly, we identified an increase of *N. meningitidis*, *E. coli*, *M. tuberculosis*, *M. kansasii* and *N. panacisegetis* in the MALAT1-deficient small intestine (Fig. 3B). In the MALAT1-deficient colon, however, there was a decrease of *Acinetobacter*, *Rhodobacteraceae*, *Varucomicrobia*, *Micrococcales* and *Sulfolobaceae*. These results suggest that the impact of MALAT1 on the intestine microbial communities is region-specific.

## MALAT1 negatively regulates polyposis in the small intestine and colon.

Previous studies reported that dysregulated intestine microbiota and altered host anti-microbial responses can modulate individual risks for developing intestine inflammation and cancer<sup>28</sup>. In human colorectal cancers, MALAT1 transcripts were downregulated relative to normal tissue<sup>29</sup>. Compared to primary Stage I lesions, MALAT1 levels were elevated in Stage IV and metastatic lesions<sup>30,31</sup>. These results suggest that MALAT1 is dynamically regulated during tumorigenesis and may contribute to multiple aspects of colorectal cancer pathogenesis in a stage-specific manner. We then tested whether MALAT1-deficiency influences disease susceptibility in a tumorigenesis setting. To address this question, we employed a mouse model of human familial adenomatous polyposis known as the APC<sup>mut</sup> line<sup>32</sup>. In this model, haploinsufficiency of the tumor suppressor APC results in hyperactivation of WNT and early onset of epithelial dysplasia<sup>33,34 32,35,36</sup>. Similar to human colorectal cancers<sup>29</sup>, MALAT1 is slightly downregulated in the murine colonic polyps compared to healthy tissues, a pattern also observed in genes encoding known colorectal cancer tumor suppressor molecules, such as *Mbd1* and *Tmigd1*<sup>37,38</sup> (Fig. 4A). To assess the role of MALAT1 in intestine tumorigenesis, we crossed the MALAT1 knockout mice to the *Apc<sup>fl/+</sup> Vil1Cre<sup>+</sup>* (APC<sup>ΔIEC</sup>) line (Fig. 4B). In the small intestine and colon, APC<sup>ΔIEC</sup> *Malat1*<sup>-/-</sup> mice harbored more polyps than MALAT1-expressing mice (Fig. 4C-D). Interestingly, the average sizes of the small intestine polyps in the APC<sup>ΔIEC</sup> *Malat1*<sup>-/-</sup> mice were smaller than those found in the MALAT1-expressing mice. These results revealed a surprising bivalent role of MALAT1 in restricting intestine polyp generation and later promoting aberrant polyp growth.

RNAs from intestine polyps and adjacent normal tissues were harvested and assessed for the expression of *Ctnnb1* encoding β-Catenin and *Ki67* as an index of cell proliferation. In the small intestine polyps and adjacent normal tissues, *Ctnnb1* and *Ki67* levels negatively correlate with the *Malat1* gene dosage (Supplementary Fig. S3-4). In contrast, expression of the tumor stem cell marker *Cd44* was MALAT1-independent. To determine the epithelial cell-intrinsic role

of MALAT1 in polyposis, we purified and cultured colonic crypt stem cells from APC<sup>ΔIEC</sup> CTL and APC<sup>ΔIEC</sup> *Malat1*<sup>-/-</sup> mice and assessed their capacity to establish colonies on Matrigel *in vitro*. Overall, APC<sup>ΔIEC</sup> *Malat1*<sup>-/-</sup> colonies were more abundant than those derived from APC<sup>ΔIEC</sup> CTL cells (Fig. 5A). Flow cytometry analysis revealed that the APC<sup>ΔIEC</sup> *Malat1*<sup>-/-</sup> cultures harbored a larger fraction of Ki67-positive actively proliferating population (Fig. 5B-C). These results suggest that MALAT1 in epithelial cells is a negative regulator of colony establishment *in vitro*.

#### MALAT1 occupies the chromatin regulatory elements on a subset of its epithelial target genes.

We hypothesized that MALAT1 suppresses polyposis in the small intestine and colon by regulating a common set of targets in both intestine regions that are involved in epithelial cell transformation. To identify these targets, we overlaid the small intestine and colon MALAT1-dependent transcripts identified from the DESeq and rMATS analysis and found 30 targets that were dependent on MALAT1 at the overall RNA expression or alternative splicing levels (Fig. 6A), including those encoding an acetylglucosaminyltransferase MGAT4C, an aldehyde dehydrogenase ALDH1A1, and an adenylate kinase AK4 that have been previously implicated in other types of cancers. In addition, two of the MALAT1 targets shared across the small intestine and colon, ZNF638 and SENP8, are associated with a change in hazards ratio for overall survival and disease-free survival in human colon adenocarcinoma patients (Fig. 6B). These results suggest that MALAT1 downstream targets may contribute to cancer pathogenesis in humans.

To determine whether these targets were regulated by MALAT1 at the chromatin level and/or through more complex mechanisms, we employed the GRID-seq assay to characterize the chromatin occupancy of MALAT1 in small intestine epithelium as previously described<sup>39,40</sup>. In the small intestine epithelium, 12 of the 30 MALAT1 target genes identified earlier had MALAT1 binding near the gene locus (Fig. 7A). For example, MALAT1 occupied the promoter/5'UTR region on *Mgat4c*, *Slc10a2*, and *Sorbs2*, intragenic regions of *Mapt*, *Tcf7l2*, and *Crem*, and distal



elements on *Zfp638*, *Rps6ka3*, *Timm23*, *Shoc2*, *Smtn*, and *Herc3* (Fig. 7B). Chromatin accessibility ATAC-seq assays further indicate that MALAT1 occupied regions in the small intestine epithelium lied within both regions of open and closed chromatin in a gene-specific manner. These results suggest that MALAT1 regulates intestine epithelial cell gene programs through both direct and indirect mechanisms.

## Discussion

MALAT1 is dysregulated in various cancer types, including colorectal cancer<sup>4,41,42</sup>. Subsequent studies reported that the expression of MALAT1 is an independent prognostic factor and is involved in tumor cell proliferation, metastasis, and epithelial-mesenchymal transition<sup>43,44</sup>. Using the APC mutant mouse model of intestine tumorigenesis, our study provides the first *in vivo* evidence that MALAT1 restricts polyp formation in both the small intestine and colon. Knocking out MALAT1 results in the generation of a larger number of intestine polyps. In addition to a role in restricting polyp formation, MALAT1 also contributes to abnormal intestinal polyp growth at a later stage. The polyps found in the MALAT1 knockout small intestine were smaller in size than those found in MALAT1-expressing mice. More detailed histological analysis in the future will be needed to determine the exact mechanism underlying MALAT1's bivalent roles in polyp initiation and growth at different disease stages.

We speculate that MALAT1 protects against polyp formation by regulating a set of target genes involved in tumorigenesis shared by both the small intestine and colon. Among the thirty MALAT1 targets commonly found in the small intestine and colon, many have been previously implicated in other types of cancers. Most interestingly, we identified two MALAT1-dependent novel molecules, ZNF638 and SENP8, that are associated with significant alterations in colon adenocarcinoma patients' overall survival and disease-free survival. One limitation of our current

transcriptomic analysis is the reliance on two pairs of control and MALAT1-deficient mice. While we have validated a few of the MALAT1-dependent IEC targets using other approaches such as flow cytometry on independent sets of mice, future transcriptomic studies powered by a larger experimental cohort will be needed to further validate these initial findings.

MALAT1 has been implicated in immune regulation, including modulating pro-inflammatory cytokine production and activating T cells and natural killer cells upon bacterial or viral infections<sup>45-47</sup>. Our findings now provide *in vivo* evidence that MALAT1 regulates anti-microbial responses in intestine epithelial cells at the levels of gene expression and alternative splicing and influences intestinal microbiome composition. Our mechanistic studies further identified MALAT1-occupied chromatin sites in the intestine epithelium genome-wide. Coupled with our transcriptomic studies, these results suggest that MALAT1 regulates intestinal epithelial gene programs by direct binding to target gene chromatin and/or indirect mechanisms. Collectively, these findings provide new insights into the function of MALAT1 in the intestine epithelium and its potential as a prognostic marker as well as a therapeutic target in intestinal diseases.

## **Materials and Methods**

### Mice

C57BL/6 wild-type were obtained from the Jackson Laboratory. *Malat1*<sup>-/-</sup> mice were obtained from Dr. David Spector's laboratory and have been previously described<sup>26</sup>. Heterozygous mice were bred to yield 8-12-week old cohoused littermates for transcriptomic and genomic studies. *Apc*<sup>fllox</sup> mice were obtained from Dr. Eric Fearon's Laboratory and previously described in reference<sup>35</sup>. Intestine tissues were harvested from 120 to 130-day-old CTL and *Malat1*<sup>-/-</sup> in the *Apc*<sup>fllox</sup> background to assess tumor burden. Tumor measurements were determined by double-blinded

analyses using ImageJ. Both male and female mice were used in the experiments described. All animal studies were approved and followed the Institutional Animal Care and Use Guidelines of the University of California San Diego (Protocol #S16156). Our vivarium at the University of California San Diego is kept under specific pathogen-free conditions. Regular serology and PCR tests are used to monitor and ensure the absence of epizootic diarrhea of infant mouse virus (EDIM), mouse hepatitis virus (MHV), mouse parvovirus (MPV), minute virus of mice (MVM), Theiler's murine encephalomyelitis virus (TMEV), fur mites and pinworms. Colonic sections from 8-week-old littermates were stained with H&E and scored for changes in the inflammatory infiltrate, submucosal inflammation, crypt morphology, and muscle thickening in a double-blind fashion as described in <sup>48</sup>.

#### Intestinal permeability assay

Mice were deprived of food and bedding for 4 hours prior to oral gavage with 4kDa Fluorescein isothiocyanate–dextran (Millipore-Sigma, FD4, 100 mg/kg) together with 70kDa Rhodamine B isothiocyanate-dextran (Millipore-Sigma, R9379, 50 mg/kg). Blood samples were taken 4 hours post-gavage by submandibular bleed. The FD4 and Rhodamine signals were measured using a TECAN fluorescent plate reader at the excitation/emission wavelengths of 485 nm/535 nm and 540 nm/585 nm, respectively.

#### Intestinal crypt isolation and organoid culture

Colonic crypts were isolated according to the manufacturer's recommendation (STEMCELL, technical bulletin #28223). Briefly, intestine tissues were harvested from 6–8-week-old CTL and *Malat1*<sup>-/-</sup> in the *Apc*<sup>fl<sup>ox</sup></sup> background and cut into 2mm pieces. After 20 washes in cold PBS, tissues were resuspended in 25mL room temperature Gentle Cell Dissociation Reagent (STEMCELL,

#07174) and incubated at room temperature for 15 minutes on a rocking platform at 20 rpm. The pellets enriched with intestinal crypts were resuspended in cold PBS containing 0.1% BSA. Isolated colonic crypts were embedded in Corning® Matrigel® Matrix (Corning™ 356231) and seeded onto pre-warmed, non-treated 24-well plates (CytoOne® by StarLab) and overlaid with conditioned media (STEMCELL, #6005) as described previously<sup>49</sup>. Organoid pictures were imaged using a Keyence bz-x800 microscope at 20X magnification with image stacks capturing the entire organoid volume.

#### Flow cytometry analysis

For analysis of tuft cells in intestinal epithelium and organoids, cells were surface stained with LIVE/DEAD Fixable Cell stain (ThermoFisher, L34957), and fluorescent conjugated antibodies against EpCAM, TGFBR1, and IL27RA (see Supplementary Table 4 for detailed information, 1:400 in PBS) for 30 minutes. For intracellular staining of Ki67, cells were first fixed/permeabilized (ThermoFisher Cat: 00-5521-00) and then incubated with the anti-Ki67 antibody for 1 hour at room temperature. Intestine epithelial cells were defined as live Epcam<sup>+</sup>. Flow cytometry data was analyzed with FlowJo (version 10.8.1).

#### cDNA synthesis and qPCR

Total RNA was extracted with the RNeasy Plus kit (QIAGEN) and reverse transcribed using iScript™ Select cDNA Synthesis Kit (Bio-Rad). Real time RT-PCR was performed using iTaq™ Universal SYBR® Green Supermix (Bio-Rad). Results were normalized to mouse *Hprt*. Primers were designed using Primer-BLAST to span across splice junctions, resulting in PCR amplicons that span at least one intron. Primer sequences are listed in Supplementary Table 4.

## RNA-seq analysis

Small intestine and colonic epithelial cells from two pairs of *Malat1*<sup>-/-</sup> and CTL cohoused littermates were enriched as previously described in <sup>48</sup>. Ribosome-depleted RNAs were used to prepare sequencing libraries. 100 bp paired-end sequencing was performed on an Illumina HiSeq4000 by the Institute of Genomic Medicine (IGM) at the University of California San Diego. Each sample yielded approximately 30-40 million reads. Paired-end reads were aligned to the mouse mm10 genome with the STAR aligner version 2.6.1a <sup>50</sup> using the parameters: "--outFilterMultimapNmax 20 --alignSJoverhangMin 8 --alignSJDBoverhangMin 1 --outFilterMismatchNmax 999 --outFilterMismatchNoverReadLmax 0.04 --alignIntronMin 20 --alignIntronMax 1000000 --alignMatesGapMax 1000000". Uniquely mapped reads overlapping with exons were counted using featureCounts <sup>51</sup> for each gene in the GENCODE.vM19 annotation. Differential expression analysis was performed using DESeq2 (v1.18.1 package) <sup>52</sup>, including a covariate in the design matrix to account for differences in harvest batch/time points. Regularized logarithm (rlog) transformation of the read counts of each gene was carried out using DESeq2. Pathway analysis was performed on differentially expressed protein coding genes with minimal counts of 10, log<sub>2</sub> fold change cutoffs of  $\geq 0.5$  or  $\leq -0.5$ , and *p*-values  $< 0.05$  using Gene Ontology (<http://www.geneontology.org/>) where all expressed genes in the specific cell type were set as background.

Alternative splicing events were analyzed by Multivariate analysis of transcript splicing (rMATS <sup>27</sup>) using the parameters "python rmats.py --b1 /path/to/b1.txt --b2 /path/to/b2.txt --gtf /path/to/the.gtf -t paired --readLength 150 --nthread 4 --od /path/to/output --tmp /path/to/tmp\_output". Using a 0.01 FDR cutoff, MALAT1-dependent splicing events were identified.

For metatranscriptomic analysis of ileal associated microbial populations, reads from the CTL and *Malat1*<sup>-/-</sup> IEC RNA-seq dataset that were not mapped to the mouse genome were

assigned with taxonomic labels using Kraken V.1. The standard Kraken database encompassing annotated bacterial, archaeal, and viral genomes was used for classification of sequences with the command: 'kraken --classified-out/path/to/classified\_fq --unclassified-out/path/to/ unclassified.fq --db \$DBNAME --paired --fastq-input pair1. fa pair2. fa > /path/to/results'. A Kraken report was generated with the the command: 'kraken-report --\$DBNAME kraken. output'<sup>53</sup>. Differential microbial counts were assessed by DEseq2 cut-off of  $p < 0.05$  with the Wald test and Log2 fold change ( $Malat1^{-}/ CTL > 1.5$  or  $\leq 1.5$ ).

### GRID-seq

GRID-seq of small intestine epithelial cells were performed as described <sup>39,40</sup>. Briefly, two independent biological replicates ( $5-10 \times 10^6$ ) were crosslinked with disuccinimidyl glutarate (DSG) and formaldehyde. DNA in isolated nuclei were digested with AluI. A biotinylated bivalent linker was ligated to chromatin-associated RNA (with the ssRNA stretch on the linker) and nearby fragmented genomic DNA and captured by streptavidin microbeads for library construction. Single-end sequencing was performed on HiSeq400 (Illumina, 200 million reads/sample). Raw sequencing reads were evaluated by FastQC <sup>54</sup>. Reads below 85bp were filtered out and those above 90bp with high quality were trimmed by Cutadapt <sup>55</sup> as suggested according to previous report <sup>39,40</sup>. The GRID-seq linker position at each read and the paired reads originated from RNA or genomic DNA were identified by matefq in GridTools <sup>39</sup>. Paired RNA and DNA reads were then mapped to the mouse genome (GRCm38/mm10) by BWA respectively. Uniquely paired reads were used to generate a set of RNA-DNA interaction matrix for downstream analyses in the GridTools pipeline. Read counts from the two repeats were summarized into two 1kb genomic bins. Chromatin enriched with MALAT1 RNAs (GRID-seq peak call) were defined as 2kb regions with clustered MALAT1 signals above the background signal expected from random interactions ( $> 5$ -fold changes).

## ATAC-seq

ATAC-seq libraries were generated as described in <sup>56</sup>. ATAC-seq processing followed the ENCODE guideline with some modifications <sup>57</sup>. Specifically, single-end raw reads were mapped to the mouse genome (GENCODE assembly mm10) by bowtie2 (Version 2.3.4.1) in the local mapping mode with parameter "--local", followed by PCR deduplication by SAMTools (Version 1.9) with the utility markedup <sup>58</sup>. Mapped reads from each sample repeats were merged into a single BAM file by SAMTools, and peaks were called using MACS2 (Version 2.2.6) <sup>59</sup> with "callpeak --nomodel --extsize 100". Regions with peak-score below 30 were filtered out and the remaining reliable peak profiles were transformed into bigwig format and visualized on the Integrative Genomics Viewer (IGV Version 2.8.2) <sup>60</sup>.

## Statistical analysis

The values are presented as the mean  $\pm$  standard deviation (SD). Statistical significance was evaluated using GraphPad Prism V.8 software (GraphPad). The t-test was used to determine significant differences between groups. A p-value of less than 0.05 was considered statistically significant in all experiments.

## **Author contributions**

T.L. designed and performed the RNA-seq experiments and analyses. J.E.H. performed the intestine permeability assays. S.M. and B.Z. performed the GRID-seq experiment and analyses. C.L. and Y.L. performed the ATAC-seq experiment and analyses. T.L. performed the polyposis and organoid experiments with help from Q.X., S.S., and microscopy support from F.T. T.L. wrote the manuscript with input from W.J.M.H.

## Acknowledgments

We thank David Spector at Cold Spring Harbor Laboratory for sharing the *Malat1*<sup>-/-</sup> mice. T.L., J.E.H., S.M., S.S, and W.J.M.H. were partially funded by the National Institutes of Health (NIH) (R01 GM124494 to WJM Huang). J.E.H. was partially funded by T32 CA067754. F.T. was funded by the National Institutes of Health (NIH) (U01DA051972). B.Z. was partially funded by the Strategic Priority Research Program of the Chinese Academy of Sciences (XDA16010113), the National Key Research and Development Program of China (2019YFA0110002 and 2019YFA0801700) and the CAS Hundred Talents Program. Illumina sequencing was conducted at the IGM Genomics Center, University of California San Diego, with support from NIH (S10 OD026929).

## Figure Legend

Fig 1. MALAT1 promotes protein-size macromolecule infiltration in the mouse intestine.

- A. Heatmap of top ten most abundantly expressed lncRNAs in the small intestine and colon epithelium isolated from two 8wk old wild-type male mice (GSE123881). Dot size indicates normalized read counts and color indicates relative expression levels of each gene among the four samples. Rep, biological replicate.
- B. Left: Breeding scheme for the generation of CTL (*Malat1*<sup>+/+</sup> or *Malat1*<sup>+/-</sup>) and *Malat1*<sup>-/-</sup> cohoused littermates employed for this study. Right: Weight of CTL (n=30) and *Malat1*<sup>-/-</sup> (n=28) mice assessed at the indicated ages. Each dot represents the result from one mouse. ns: no significant (t-test).
- C. Representative H&E staining of colonic sections from two pairs of 12-week-old CTL and *Malat1*<sup>-/-</sup> female mice.
- D. Colon crypt height, density, and overall histology scores from CTL (n=3) and *Malat1*<sup>-/-</sup> (n=4) mice. n.s. not significant (t-test).



- E. Quantification of FITC-dextran and RITC-dextran in serum from CTL (n=5) and *Malat1*<sup>-/-</sup> (n=3) mice. Each dot represents the result from one mouse.
- \* p-value<0.05, n.s. not significant (t-test).

Fig 2. MALAT1 regulates select intestine epithelial cell RNA abundance and splicing.

- A. Distribution of MALAT1-dependent genes in the small intestine and colon IECs as determined by DESeq2 in two pairs of cohoused CTL and *Malat1*<sup>-/-</sup> littermates (12-week-old females).
- B. Distribution of small intestine and colon transcripts relying on MALAT1 for alternative splicing as determined by rMATS in two pairs of cohoused CTL and *Malat1*<sup>-/-</sup> littermates (12-week-old females).

Fig 3. MALAT1-dependent mucosal-associated microbes in the intestine.

- A. Gene ontology enrichment analysis of the small intestine and colon epithelium MALAT1 targets from DESeq2 and rMATS combined. The size of the dot is proportional to the number of genes mapping to the enriched GO term.
- B. Volcano plots of meta-transcriptomic analysis of small intestine and colon IEC RNA-seq data from two pairs of cohoused CTL and *Malat1*<sup>-/-</sup> littermates (12-week-old females).

Fig 4. MALAT1 negatively regulates polyposis in the small intestine and colon.

- A. Normalized read counts of MALAT1 and select genes encoding known tumor suppressors in colorectal cancer in the steady state colonic epithelium and colonic polyps from the *APC*<sup>ΔIEC</sup> mice (GSE146014).
- B. Experimental scheme of *APC*<sup>ΔIEC</sup> CTL and *APC*<sup>ΔIEC</sup> *Malat1*<sup>-/-</sup> mice.

- C. Polyp count and average polyp diameter in the small intestine (combined counts of the duodenum, jejunum, and ileum) and colon of 120-day old  $APC^{\Delta IEC}$  CTL (circle, n=7) and  $APC^{\Delta IEC} Malat1^{-/-}$  mice (triangle, n=7). Each dot represents the results from one mouse. Open circles/triangles indicate the results from the tissues shown in Fig. 3D.
- \* p-value<0.05, \*\* p-value<0.01, n.s. not significant (t-test).
- D. Representative bright-field images of tumor-bearing small intestine and colons from a pair of  $APC^{\Delta cIEC}$  CTL and  $APC^{\Delta cIEC} Malat1^{-/-}$  mice from C. Scale bar equals 1 cm.

Fig. 5 MALAT1 promotes intestine organoid colony formation and proliferation.

- A. Representative brightfield images of organoids derived from  $APC^{\Delta IEC}$  CTL and  $APC^{\Delta IEC} Malat1^{-/-}$  colonic crypt stem cells. Scale bar represents 200 $\mu$ m.
- B. Representative flow cytometry analysis of intracellular Ki67 staining in live  $APC^{\Delta IEC}$  CTL and  $APC^{\Delta IEC} Malat1^{-/-}$  colonic organoid cells (Live Epcam<sup>+</sup>). SSC: side scatter as an index for cell granularity.
- C. The proportion of Ki67<sup>+</sup> colonic organoid cells in the  $APC^{\Delta IEC}$  CTL and  $APC^{\Delta IEC} Malat1^{-/-}$  cultures. Each dot represents the result from one independent experiment.
- \* p-value<0.05 (t-test).

Fig 6. Select MALAT1-dependent genes in predicting colorectal cancer patient hazard risks.

- A. Overlap analysis of the differential expressed genes and MALAT1-dependent splicing events in the small intestine and colon. RI: retained intron. SE: skipped exon. A5SS: alternative 5' splice site. A3SS: alternative 3' splice site.
- B. Overall survival and disease-free survival among colon adenocarcinoma patients with high or low expression of each MALAT1 target identified in A.

Fig 7. MALAT1 occupies the chromatin regulatory elements on a subset of its epithelial target genes.

- A. Venn diagrams of overlapping differential expressed genes and MALAT1-dependent splicing events between small and large intestine. Black: MALAT1 chromatin occupancy detected at or near the gene body. Grey: MALAT1 not recruited to nearby chromatin.
- B. IGV browser views of MALAT1 GRID-seq and open chromatin (ATAC-seq) signals on select MALAT1-direct target genes from A <sup>61</sup>. Rep, biological replicate.

Supplementary Fig. S1. MALAT1-dependent target validation.

- A. IGV browser views of CTL (black) and *Malat1*<sup>-/-</sup> (grey) RNA-seq signals at the *Tgfb1* locus. Connecting lines indicate reads spanning exon junctions.
- B. The proportion of TGFBR1-expressing small intestine epithelial cells (Epcam<sup>+</sup>) in three pairs of 12-week-old CTL and *Malat1*<sup>-/-</sup> littermates as determined by flow cytometry. Each dot represents the result from one mouse. \* p-value<0.05 (t-test).
- C. IGV browser views of CTL (black) and *Malat1*<sup>-/-</sup> (grey) RNA-seq signals at the *Il27ra* locus. Connecting lines indicate reads spanning exon junctions.
- D. The proportion of IL-27RA-expressing colonic epithelial cells (Epcam<sup>+</sup>) from two pairs of 12-week-old CTL and *Malat1*<sup>-/-</sup> littermates as determined by flow cytometry. Each dot represents the result from one mouse. \* p-value<0.05 (t-test).

Supplementary Fig. S2. MALAT1-dependent genes involved in response to bacteria.

- A. MALAT1-dependent gene network in the small intestine and colonic epithelium. Each orange dot represents one gene and blue nodes indicate pathway annotation. The color

of the nodes represents the number of MALAT1-dependent genes associated with the specific annotation term and the size of the node represents the  $-\log_{10}(\text{adjusted p-value})$ .

Supplementary Fig. S3. Select small intestine gene expression in the polyposis model.

A. *Ctnnb1*, *Ki67*, and *Cd44* mRNA expression in ileal polyps and adjacent normal tissues from  $APC^{\Delta IE C} Malat1^{+/+}$  (n=3),  $Malat1^{+/-}$  (n=5), and  $Malat1^{-/-}$  (n=7) mice harvested on day 120. Levels were normalized to housekeeping gene *Hprt*. Adj Norm, adjacent normal tissue. \*, p-value<0.05, n.s. not significant (Welch's t-test).

Supplementary Fig. S4. Select colonic gene expression in the polyposis model.

A. *Ctnnb1*, *Ki67*, and *Cd44* mRNA expression in colonic polyps and adjacent normal tissues from  $APC^{\Delta IE C} Malat1^{+/+}$  (n=2),  $Malat1^{+/-}$  (n=3), and  $Malat1^{-/-}$  (n=5) mice harvested on day 120. Levels were normalized to housekeeping gene *Hprt*. Adj Norm, adjacent normal tissue. n.s. not significant (Welch's t-test).

## References

- 1 Ali, A., Tan, H. & Kaiko, G. E. Role of the Intestinal Epithelium and Its Interaction With the Microbiota in Food Allergy. *Frontiers in Immunology* **11**, doi:10.3389/fimmu.2020.604054 (2020).
- 2 Zhu, M. & Xie, J. LncRNA MALAT1 Promotes Ulcerative Colitis by Upregulating IncRNA ANRIL. *Digestive diseases and sciences* **65**, 3191-3196, doi:10.1007/s10620-020-06093-w (2020).
- 3 Zheng, H. T. *et al.* High expression of lncRNA MALAT1 suggests a biomarker of poor prognosis in colorectal cancer. *International journal of clinical and experimental pathology* **7**, 3174-3181 (2014).
- 4 Li, P. *et al.* MALAT1 Is Associated with Poor Response to Oxaliplatin-Based Chemotherapy in Colorectal Cancer Patients and Promotes Chemoresistance through EZH2. *Molecular cancer therapeutics* **16**, 739-751, doi:10.1158/1535-7163.Mct-16-0591 (2017).
- 5 Li, Q., Dai, Y., Wang, F. & Hou, S. Differentially expressed long non-coding RNAs and the prognostic potential in colorectal cancer. *Neoplasma* **63**, 977-983, doi:10.4149/neo\_2016\_617 (2016).
- 6 Li, Y. *et al.* MALAT1 Maintains the Intestinal Mucosal Homeostasis in Crohn's Disease via the miR-146b-5p-CLDN11/NUMB Pathway. *Journal of Crohn's and Colitis* **15**, 1542-1557, doi:10.1093/ecco-jcc/jjab040 (2021).
- 7 Wang, H. *et al.* MALAT1/miR-101-3p/MCL1 axis mediates cisplatin resistance in lung cancer. *Oncotarget* **9**, 7501-7512, doi:10.18632/oncotarget.23483 (2018).
- 8 Gong, W. J. *et al.* Association of well-characterized lung cancer lncRNA polymorphisms with lung cancer susceptibility and platinum-based chemotherapy response. *Tumour*

- biology : the journal of the International Society for Oncodevelopmental Biology and Medicine* **37**, 8349-8358, doi:10.1007/s13277-015-4497-5 (2016).
- 9 Chou, J. *et al.* MALAT1 induced migration and invasion of human breast cancer cells by competitively binding miR-1 with cdc42. *Biochemical and biophysical research communications* **472**, 262-269, doi:10.1016/j.bbrc.2016.02.102 (2016).
- 10 Westphalen, C. B., Quante, M. & Wang, T. C. Functional implication of Dclk1 and Dclk1-expressing cells in cancer. *Small GTPases* **8**, 164-171, doi:10.1080/21541248.2016.1208792 (2017).
- 11 Wu, L., Wang, X. & Guo, Y. Long non-coding RNA MALAT1 is upregulated and involved in cell proliferation, migration and apoptosis in ovarian cancer. *Experimental and therapeutic medicine* **13**, 3055-3060, doi:10.3892/etm.2017.4304 (2017).
- 12 Stamato, M. A. *et al.* Inhibition of EZH2 triggers the tumor suppressive miR-29b network in multiple myeloma. *Oncotarget* **8**, 106527-106537, doi:10.18632/oncotarget.22507 (2017).
- 13 Wang, W. *et al.* Long noncoding RNA MALAT1 promotes malignant development of esophageal squamous cell carcinoma by targeting  $\beta$ -catenin via Ezh2. *Oncotarget* **7**, 25668-25682, doi:10.18632/oncotarget.8257 (2016).
- 14 Wang, X. *et al.* Silencing of long noncoding RNA MALAT1 by miR-101 and miR-217 inhibits proliferation, migration, and invasion of esophageal squamous cell carcinoma cells. *The Journal of biological chemistry* **290**, 3925-3935, doi:10.1074/jbc.M114.596866 (2015).
- 15 Guo, F. *et al.* Inhibition of metastasis-associated lung adenocarcinoma transcript 1 in CaSki human cervical cancer cells suppresses cell proliferation and invasion. *Acta biochimica et biophysica Sinica* **42**, 224-229, doi:10.1093/abbs/gmq008 (2010).
- 16 Yang, L., Bai, H. S., Deng, Y. & Fan, L. High MALAT1 expression predicts a poor prognosis of cervical cancer and promotes cancer cell growth and invasion. *European review for medical and pharmacological sciences* **19**, 3187-3193 (2015).

- 17 Xia, H. *et al.* The lncRNA MALAT1 is a novel biomarker for gastric cancer metastasis. *Oncotarget* **7**, 56209-56218, doi:10.18632/oncotarget.10941 (2016).
- 18 Ji, P. *et al.* MALAT-1, a novel noncoding RNA, and thymosin beta4 predict metastasis and survival in early-stage non-small cell lung cancer. *Oncogene* **22**, 8031-8041, doi:10.1038/sj.onc.1206928 (2003).
- 19 Tripathi, V. *et al.* The nuclear-retained noncoding RNA MALAT1 regulates alternative splicing by modulating SR splicing factor phosphorylation. *Molecular cell* **39**, 925-938, doi:10.1016/j.molcel.2010.08.011 (2010).
- 20 Miyagawa, R. *et al.* Identification of cis- and trans-acting factors involved in the localization of MALAT-1 noncoding RNA to nuclear speckles. *RNA (New York, N.Y.)* **18**, 738-751, doi:10.1261/rna.028639.111 (2012).
- 21 Yang, L. *et al.* ncRNA- and Pc2 methylation-dependent gene relocation between nuclear structures mediates gene activation programs. *Cell* **147**, 773-788, doi:10.1016/j.cell.2011.08.054 (2011).
- 22 Engreitz, J. M. *et al.* RNA-RNA interactions enable specific targeting of noncoding RNAs to nascent Pre-mRNAs and chromatin sites. *Cell* **159**, 188-199, doi:10.1016/j.cell.2014.08.018 (2014).
- 23 Salmena, L., Poliseno, L., Tay, Y., Kats, L. & Pandolfi, P. P. A ceRNA hypothesis: the Rosetta Stone of a hidden RNA language? *Cell* **146**, 353-358, doi:10.1016/j.cell.2011.07.014 (2011).
- 24 Chang, S. M. & Hu, W. W. Long non-coding RNA MALAT1 promotes oral squamous cell carcinoma development via microRNA-125b/STAT3 axis. *Journal of cellular physiology* **233**, 3384-3396, doi:10.1002/jcp.26185 (2018).
- 25 Luan, W. *et al.* Long non-coding RNA MALAT1 acts as a competing endogenous RNA to promote malignant melanoma growth and metastasis by sponging miR-22. *Oncotarget* **7**, 63901-63912, doi:10.18632/oncotarget.11564 (2016).

- 26 Zhang, B. *et al.* The lncRNA Malat1 is dispensable for mouse development but its transcription plays a cis-regulatory role in the adult. *Cell Rep* **2**, 111-123, doi:10.1016/j.celrep.2012.06.003 (2012).
- 27 Shen, S. *et al.* rMATS: robust and flexible detection of differential alternative splicing from replicate RNA-Seq data. *Proc Natl Acad Sci U S A* **111**, E5593-5601, doi:10.1073/pnas.1419161111 (2014).
- 28 Louis, P., Hold, G. L. & Flint, H. J. The gut microbiota, bacterial metabolites and colorectal cancer. *Nat Rev Microbiol* **12**, 661-672, doi:10.1038/nrmicro3344 (2014).
- 29 Kwok, Z. H., Roche, V., Chew, X. H., Fadieieva, A. & Tay, Y. A non-canonical tumor suppressive role for the long non-coding RNA MALAT1 in colon and breast cancers. *Int J Cancer* **143**, 668-678, doi:10.1002/ijc.31386 (2018).
- 30 Zhang, C. *et al.* Long Noncoding RNA MALAT1 Promotes Colorectal Cancer Progression by Acting as a ceRNA of miR-508-5p to Regulate RAB14 Expression. *Biomed Res Int* **2020**, 4157606, doi:10.1155/2020/4157606 (2020).
- 31 Ji, Q. *et al.* MALAT1 regulates the transcriptional and translational levels of proto-oncogene RUNX2 in colorectal cancer metastasis. *Cell Death Dis* **10**, 378, doi:10.1038/s41419-019-1598-x (2019).
- 32 Kwong, L. N. & Dove, W. F. APC and its modifiers in colon cancer. *Adv Exp Med Biol* **656**, 85-106 (2009).
- 33 Hinoi, T. *et al.* Mouse model of colonic adenoma-carcinoma progression based on somatic *Apc* inactivation. *Cancer Res* **67**, 9721-9730, doi:10.1158/0008-5472.CAN-07-2735 (2007).
- 34 Wang, K. *et al.* Interleukin-17 receptor signaling in transformed enterocytes promotes early colorectal tumorigenesis. *Immunity* **41**, 1052-1063, doi:10.1016/j.immuni.2014.11.009 (2014).



- 35 Grivennikov, S. I. *et al.* Adenoma-linked barrier defects and microbial products drive IL-23/IL-17-mediated tumour growth. *Nature* **491**, 254-258, doi:10.1038/nature11465 (2012).
- 36 Fodde, R. *et al.* A targeted chain-termination mutation in the mouse *Apc* gene results in multiple intestinal tumors. *Proc Natl Acad Sci U S A* **91**, 8969-8973 (1994).
- 37 Qi, L. & Ding, Y. Screening of Tumor Suppressor Genes in Metastatic Colorectal Cancer. *Biomed Res Int* **2017**, 2769140, doi:10.1155/2017/2769140 (2017).
- 38 Mu, L. *et al.* The Role of TMIGD1 as a Tumor Suppressor in Colorectal Cancer. *Genet Test Mol Biomarkers* **26**, 174-183, doi:10.1089/gtmb.2021.0169 (2022).
- 39 Zhou, B. *et al.* GRID-seq for comprehensive analysis of global RNA-chromatin interactions. *Nat Protoc* **14**, 2036-2068, doi:10.1038/s41596-019-0172-4 (2019).
- 40 Li, X. *et al.* GRID-seq reveals the global RNA-chromatin interactome. *Nat Biotechnol* **35**, 940-950, doi:10.1038/nbt.3968 (2017).
- 41 Arun, G., Aggarwal, D. & Spector, D. L. MALAT1 Long Non-Coding RNA: Functional Implications. *Non-Coding RNA* **6**, 22 (2020).
- 42 Wei, Y. & Niu, B. Role of MALAT1 as a Prognostic Factor for Survival in Various Cancers: A Systematic Review of the Literature with Meta-Analysis. *Disease markers* **2015**, 164635, doi:10.1155/2015/164635 (2015).
- 43 Sun, Z. *et al.* YAP1-induced MALAT1 promotes epithelial–mesenchymal transition and angiogenesis by sponging miR-126-5p in colorectal cancer. *Oncogene* **38**, 2627-2644, doi:10.1038/s41388-018-0628-y (2019).
- 44 Ji, Q. *et al.* Long non-coding RNA MALAT1 promotes tumour growth and metastasis in colorectal cancer through binding to SFPQ and releasing oncogene PTBP2 from SFPQ/PTBP2 complex. *Br J Cancer* **111**, 736-748, doi:10.1038/bjc.2014.383 (2014).
- 45 Kakaradov, B. *et al.* Early transcriptional and epigenetic regulation of CD8<sup>+</sup> T cell differentiation revealed by single-cell RNA sequencing. *Nature Immunology* **18**, 422-432, doi:10.1038/ni.3688 (2017).

- 46 Kanbar, J. N. *et al.* The long noncoding RNA Malat1 regulates CD8+ T cell differentiation by mediating epigenetic repression. *Journal of Experimental Medicine* **219**, e20211756, doi:10.1084/jem.20211756 (2022).
- 47 Kim, S. H., Kim, S. H., Yang, W. I., Kim, S. J. & Yoon, S. O. Association of the long non-coding RNA MALAT1 with the polycomb repressive complex pathway in T and NK cell lymphoma. *Oncotarget* **8**, 31305-31317, doi:10.18632/oncotarget.15453 (2017).
- 48 Abbasi, N. *et al.* DDX5 promotes oncogene C3 and FABP1 expressions and drives intestinal inflammation and tumorigenesis. *Life Sci Alliance* **3**, doi:10.26508/lsa.202000772 (2020).
- 49 Miyoshi, H. & Stappenbeck, T. S. In vitro expansion and genetic modification of gastrointestinal stem cells in spheroid culture. *Nature protocols* **8**, 2471-2482, doi:10.1038/nprot.2013.153 (2013).
- 50 Dobin, A. *et al.* STAR: ultrafast universal RNA-seq aligner. *Bioinformatics* **29**, 15-21, doi:10.1093/bioinformatics/bts635 (2013).
- 51 Liao, Y., Smyth, G. K. & Shi, W. featureCounts: an efficient general purpose program for assigning sequence reads to genomic features. *Bioinformatics* **30**, 923-930, doi:10.1093/bioinformatics/btt656 (2014).
- 52 Love, M. I., Huber, W. & Anders, S. Moderated estimation of fold change and dispersion for RNA-seq data with DESeq2. *Genome Biol* **15**, 550, doi:10.1186/s13059-014-0550-8 (2014).
- 53 Wood, D. E. & Salzberg, S. L. Kraken: ultrafast metagenomic sequence classification using exact alignments. *Genome Biology* **15**, R46, doi:10.1186/gb-2014-15-3-r46 (2014).
- 54 Gu, Z., Gu, L., Eils, R., Schlesner, M. & Brors, B. circlize Implements and enhances circular visualization in R. *Bioinformatics* **30**, 2811-2812, doi:10.1093/bioinformatics/btu393 (2014).

- 55 Martin, M. Cutadapt removes adapter sequences from high-throughput sequencing reads. *2011* **17**, 3, doi:10.14806/ej.17.1.200 (2011).
- 56 Buenrostro, J. D., Wu, B., Chang, H. Y. & Greenleaf, W. J. ATAC-seq: A Method for Assaying Chromatin Accessibility Genome-Wide. *Curr Protoc Mol Biol* **109**, 21 29 21-21 29 29, doi:10.1002/0471142727.mb2129s109 (2015).
- 57 Landt, S. G. *et al.* ChIP-seq guidelines and practices of the ENCODE and modENCODE consortia. *Genome Res* **22**, 1813-1831, doi:10.1101/gr.136184.111 (2012).
- 58 Li, H. *et al.* The Sequence Alignment/Map format and SAMtools. *Bioinformatics* **25**, 2078-2079, doi:10.1093/bioinformatics/btp352 (2009).
- 59 Zhang, Y. *et al.* Model-based analysis of ChIP-Seq (MACS). *Genome Biol* **9**, R137, doi:10.1186/gb-2008-9-9-r137 (2008).
- 60 Thorvaldsdottir, H., Robinson, J. T. & Mesirov, J. P. Integrative Genomics Viewer (IGV): high-performance genomics data visualization and exploration. *Brief Bioinform* **14**, 178-192, doi:10.1093/bib/bbs017 (2013).
- 61 Tang, Z. *et al.* GEPIA: a web server for cancer and normal gene expression profiling and interactive analyses. *Nucleic Acids Res* **45**, W98-W102, doi:10.1093/nar/gkx247 (2017).

**Fig 1. MALAT1 promotes protein-size macromolecule infiltration in the mouse intestine.**

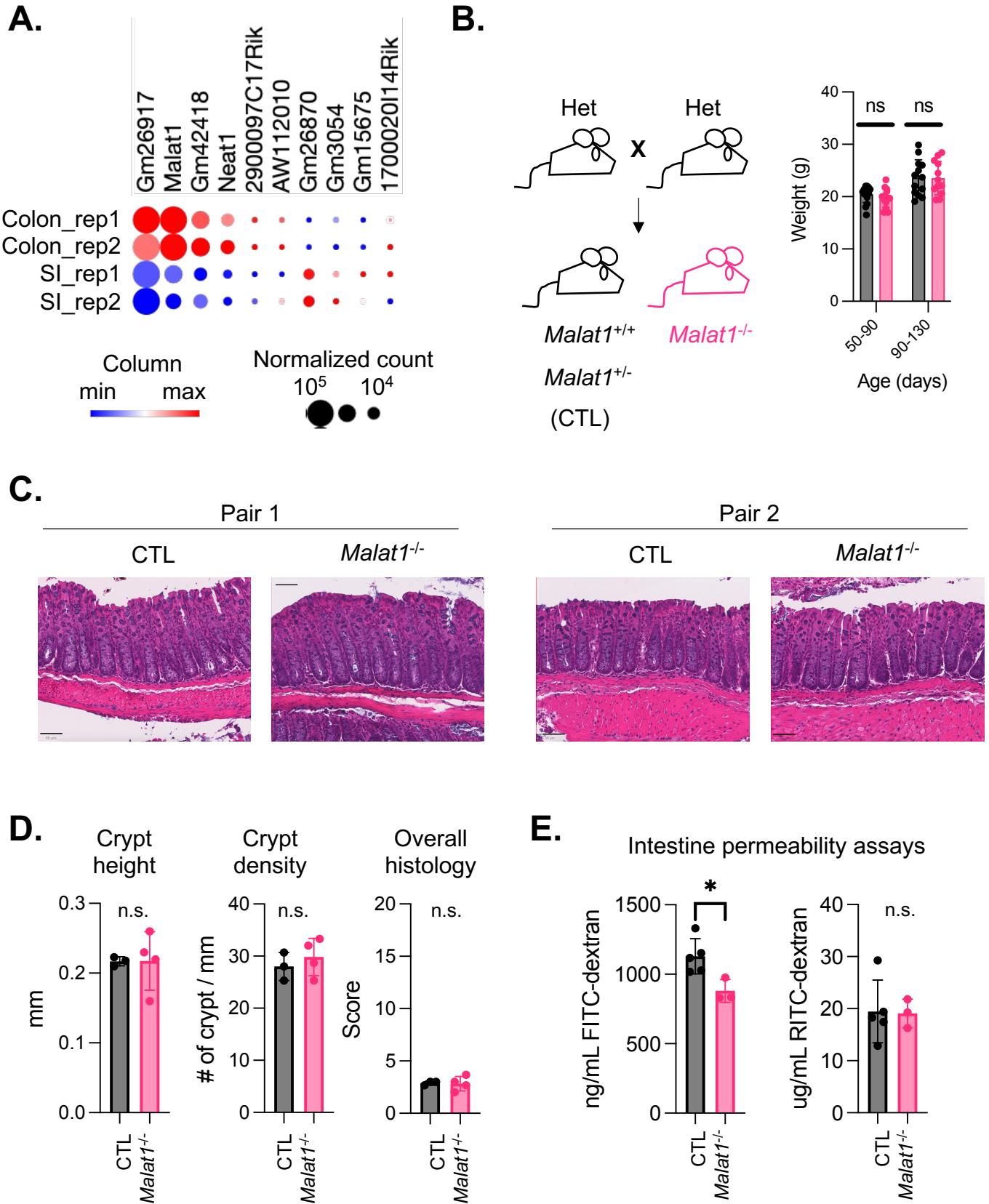
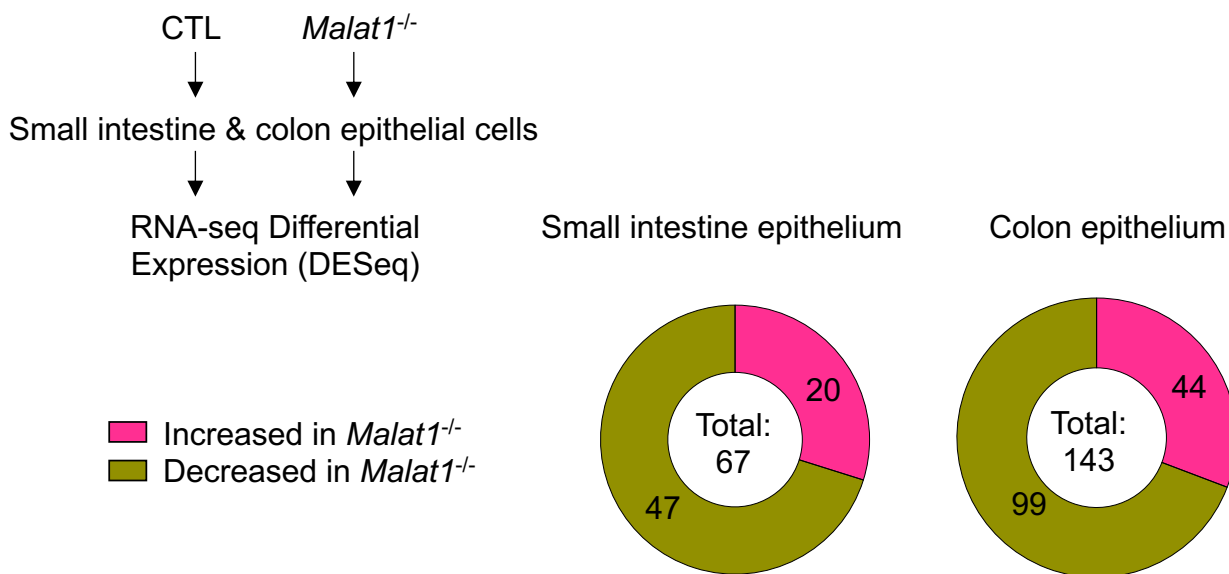


**Fig 2. MALAT1 regulates select intestine epithelial cell RNA abundance and splicing.**

**A.**



**B.**

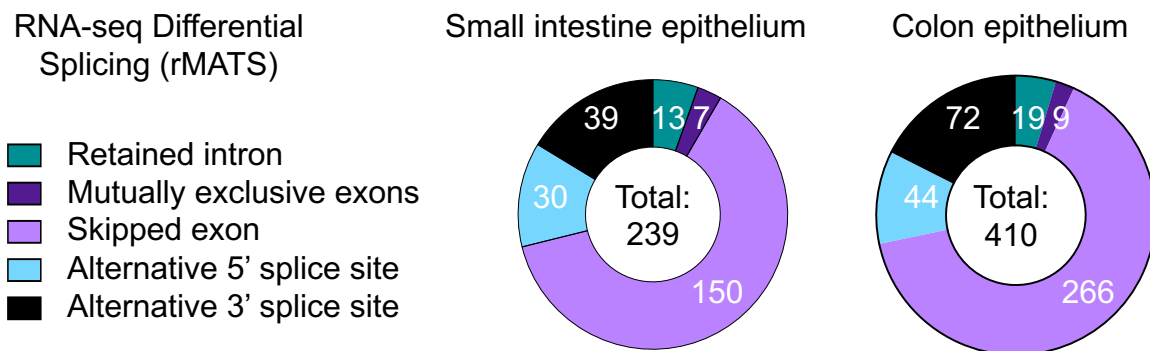
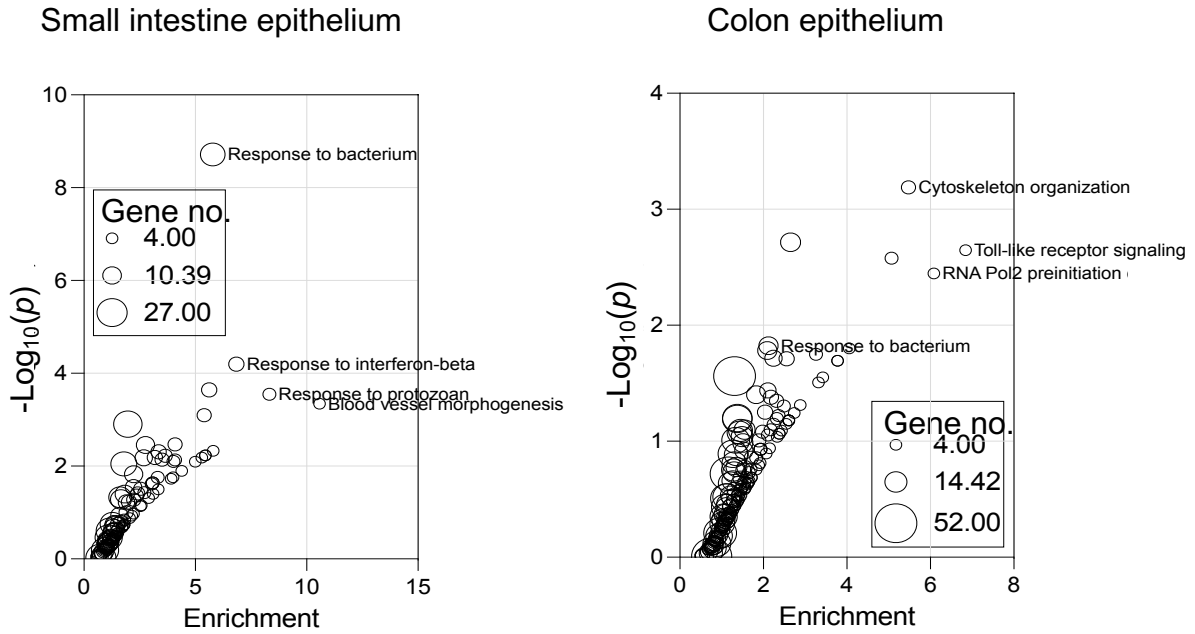
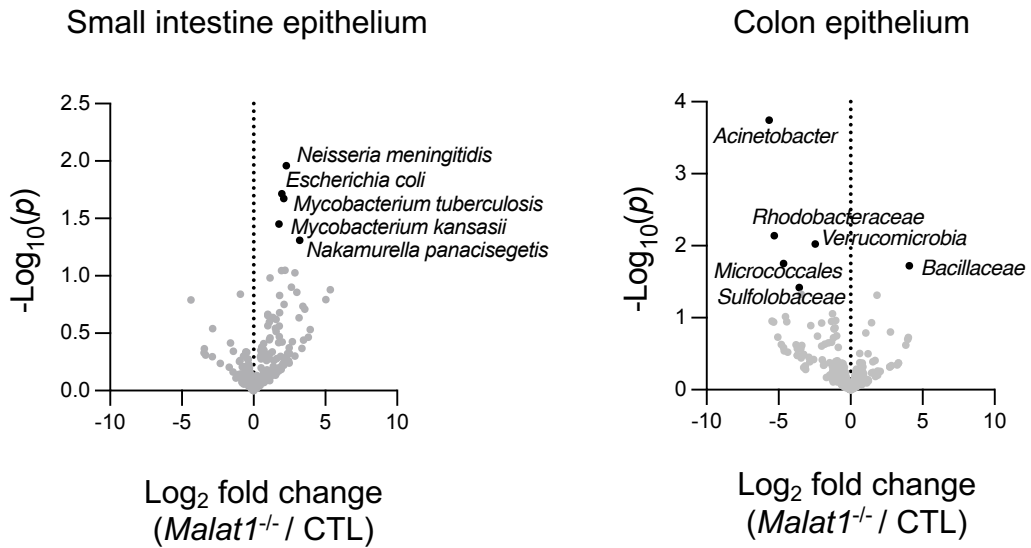


Fig 3. MALAT1-dependent mucosal associated microbes in the intestine.

**A.**



**B.**



**Fig 4. MALAT1 negatively regulates polyposis in the small intestine and colon.**

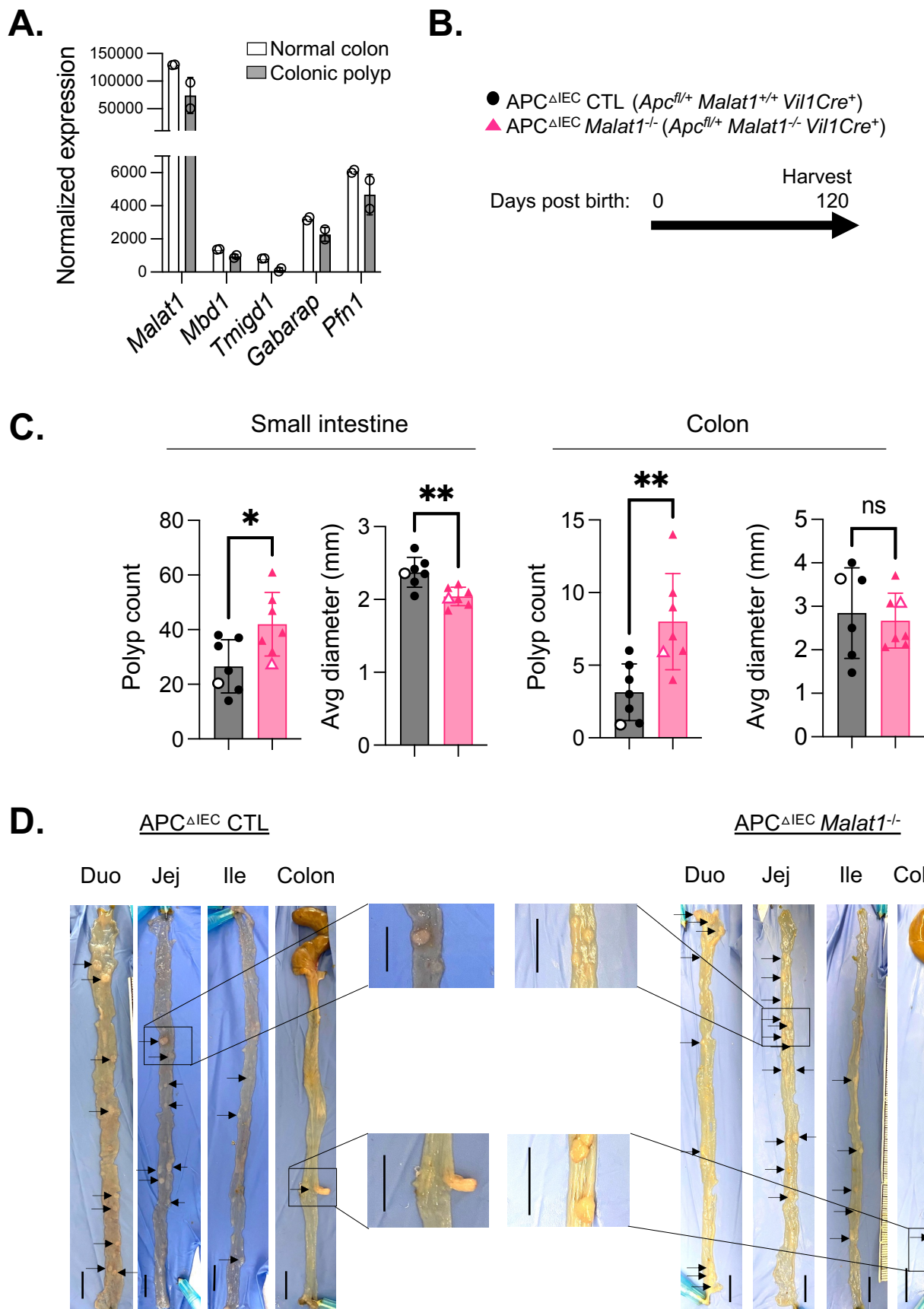
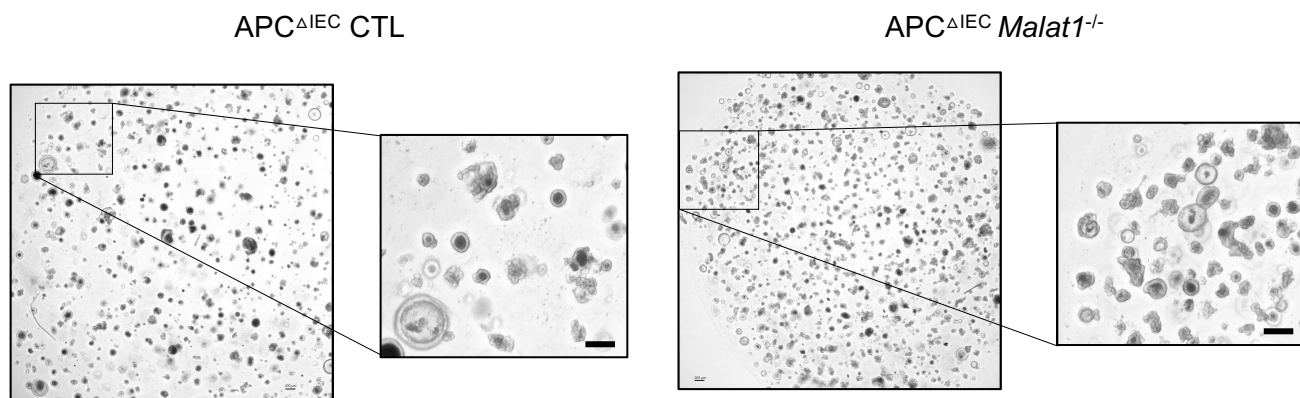
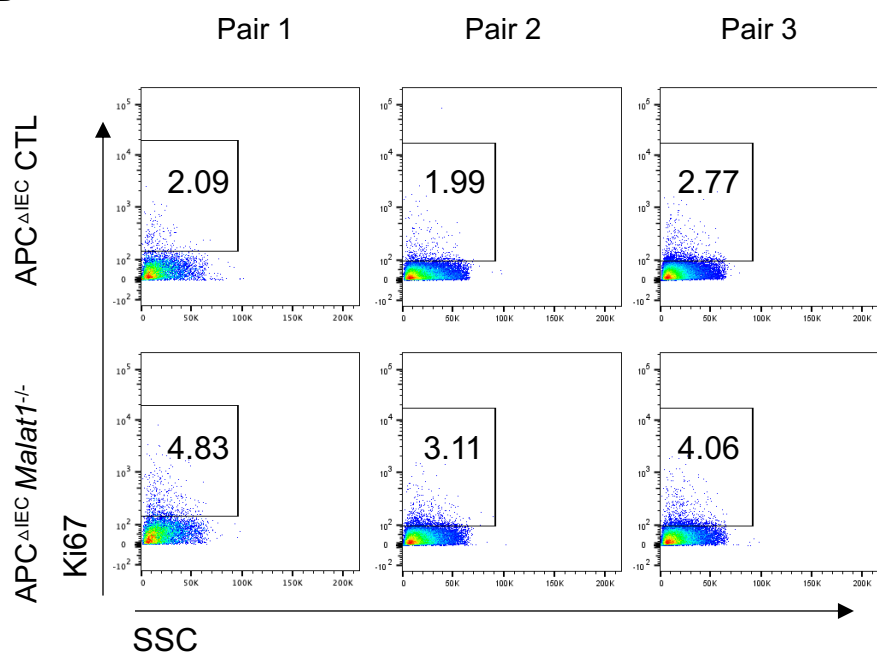


Fig 5. MALAT1 promotes intestine organoid colony formation and proliferation.

**A**



**B**



**C**

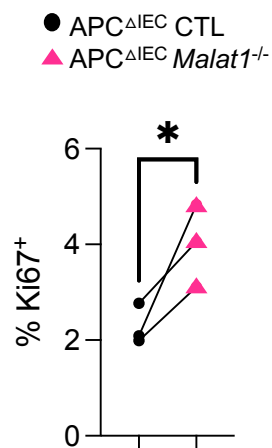




**Fig 6. Select MALAT1-dependent genes in predicting colorectal cancer patient hazard risks.**

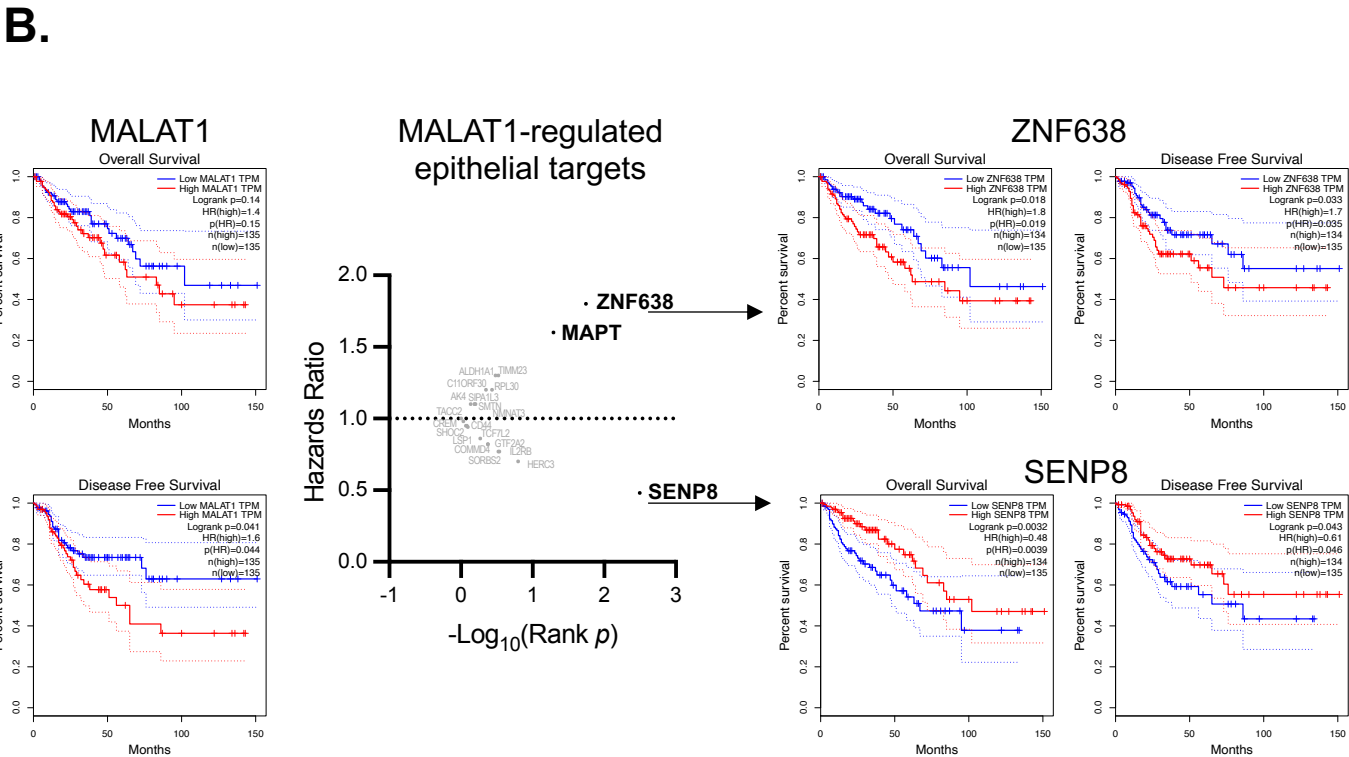
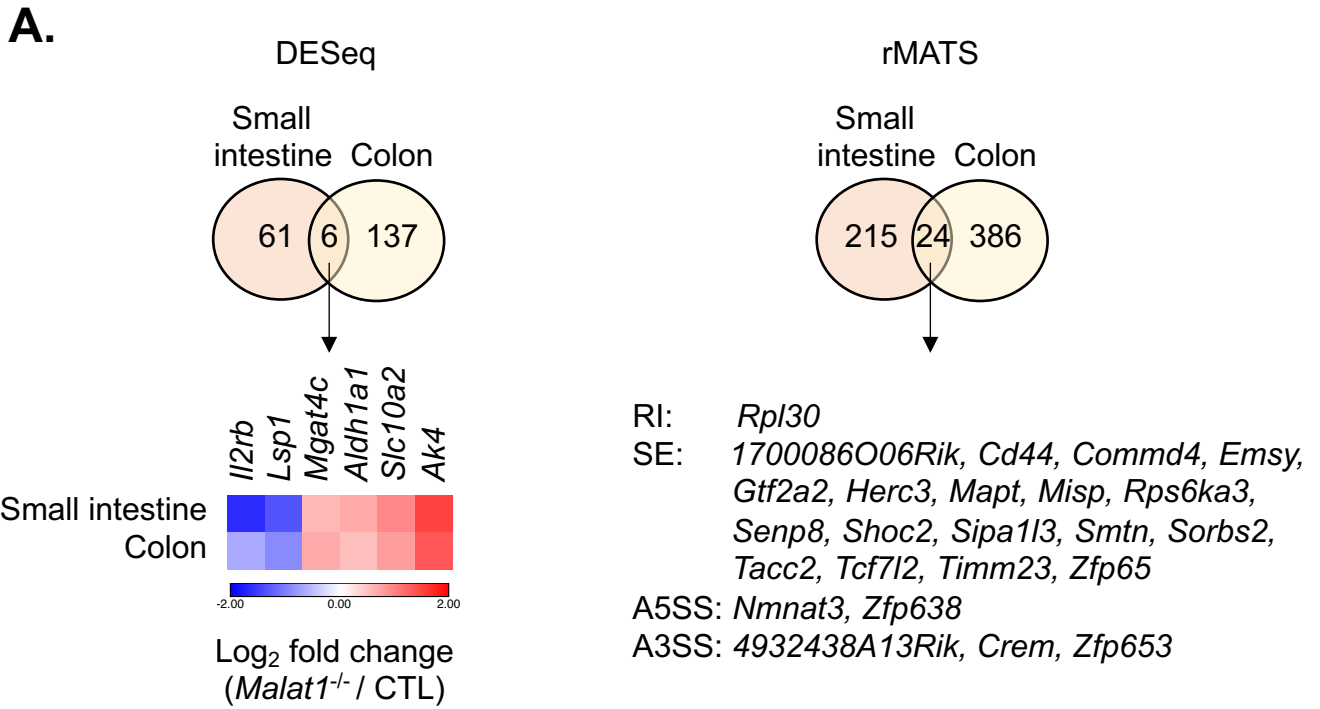
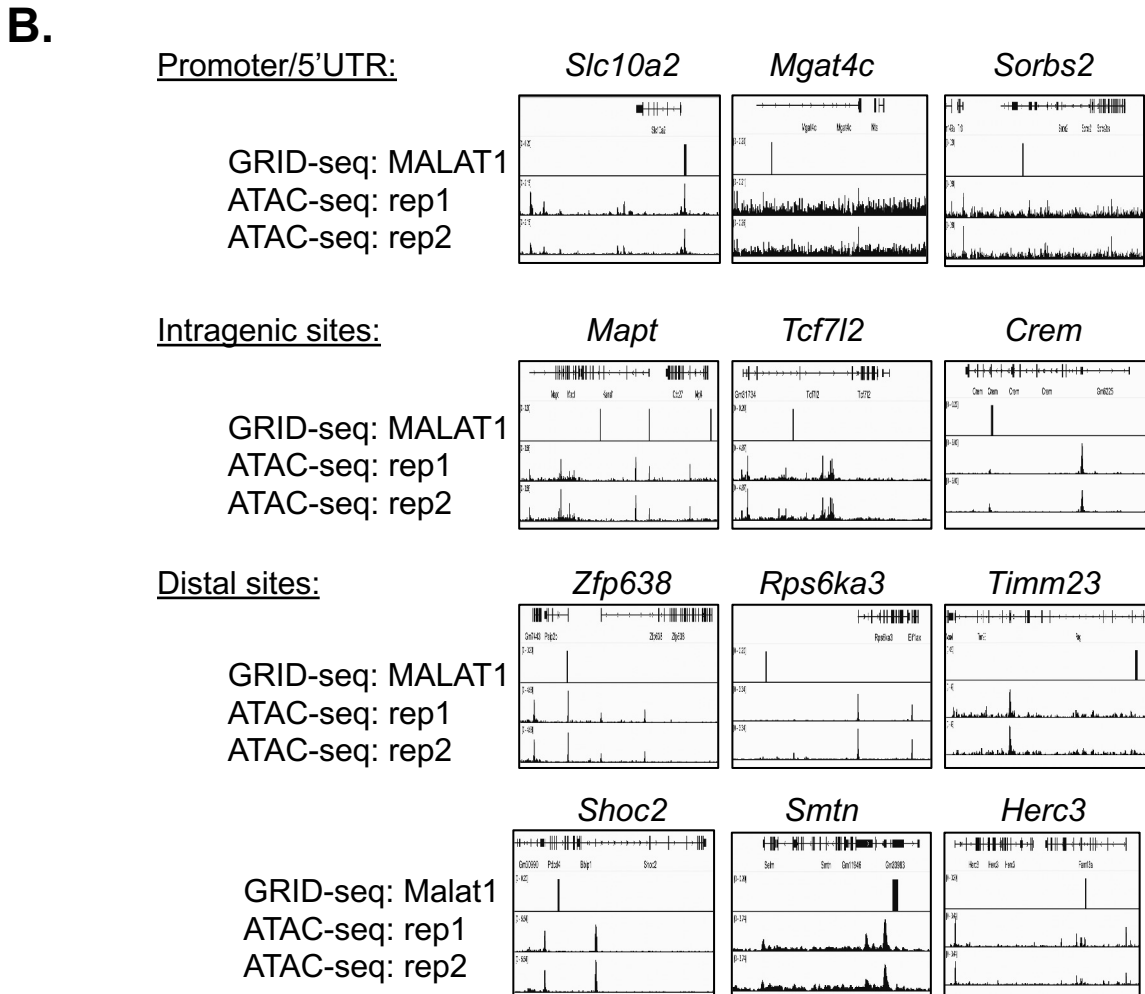
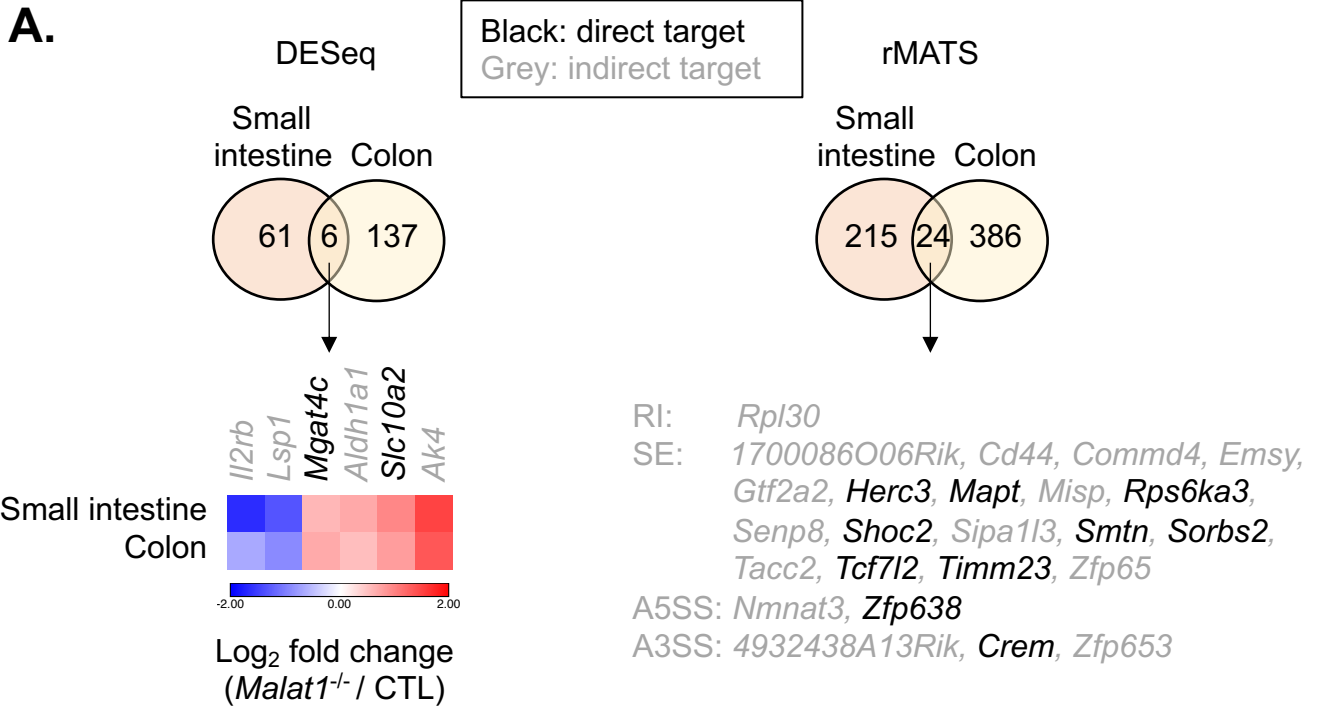
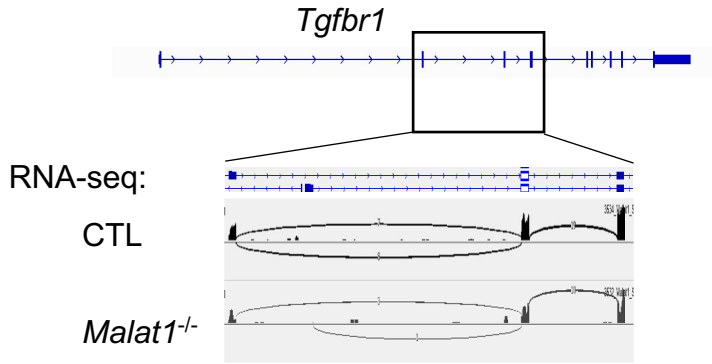


**Fig 7. MALAT1 occupies the chromatin regulatory elements on a subset of its epithelial target genes.**

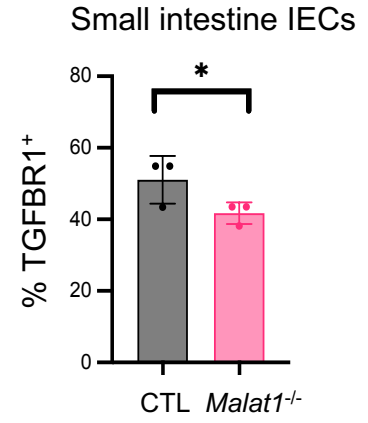


Supplementary Fig S1. MALAT1-dependent target validation.

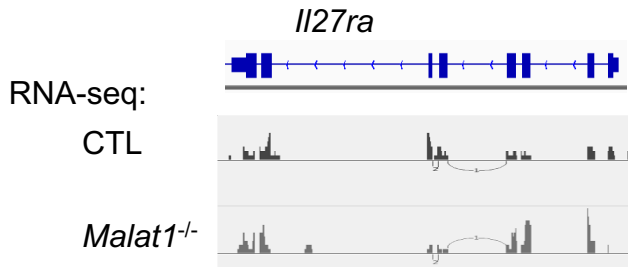
**A.**



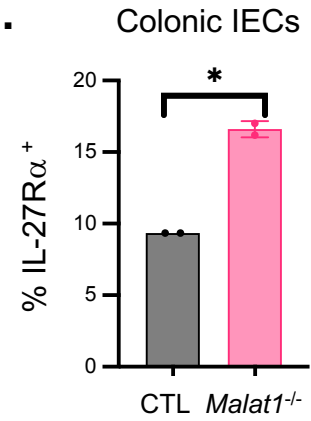
**B.**



**C.**



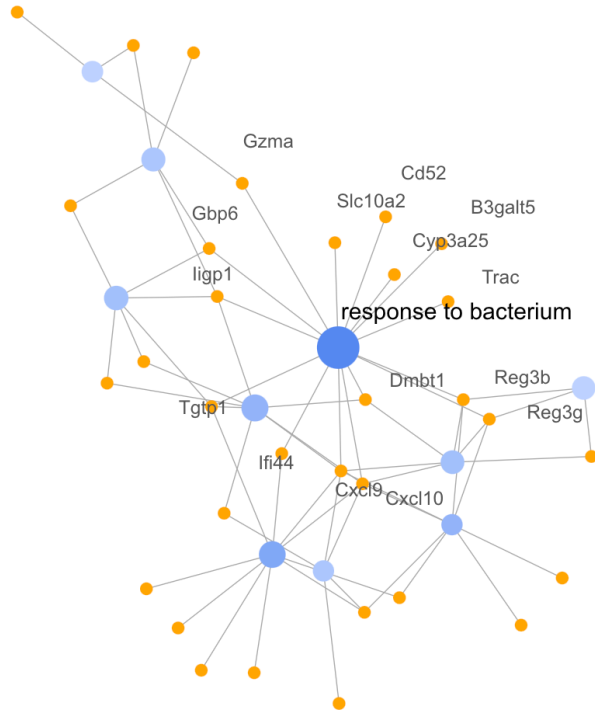
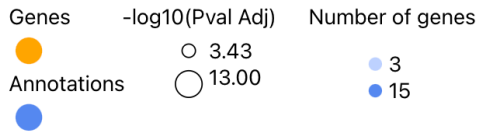
**D.**



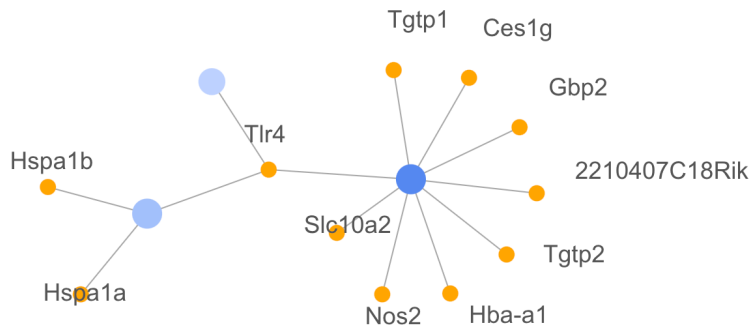
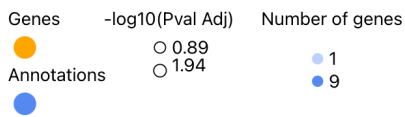
# Supplementary Fig S2. MALAT1-dependent genes involved in response to bacteria.

**A**

## Small Intestine

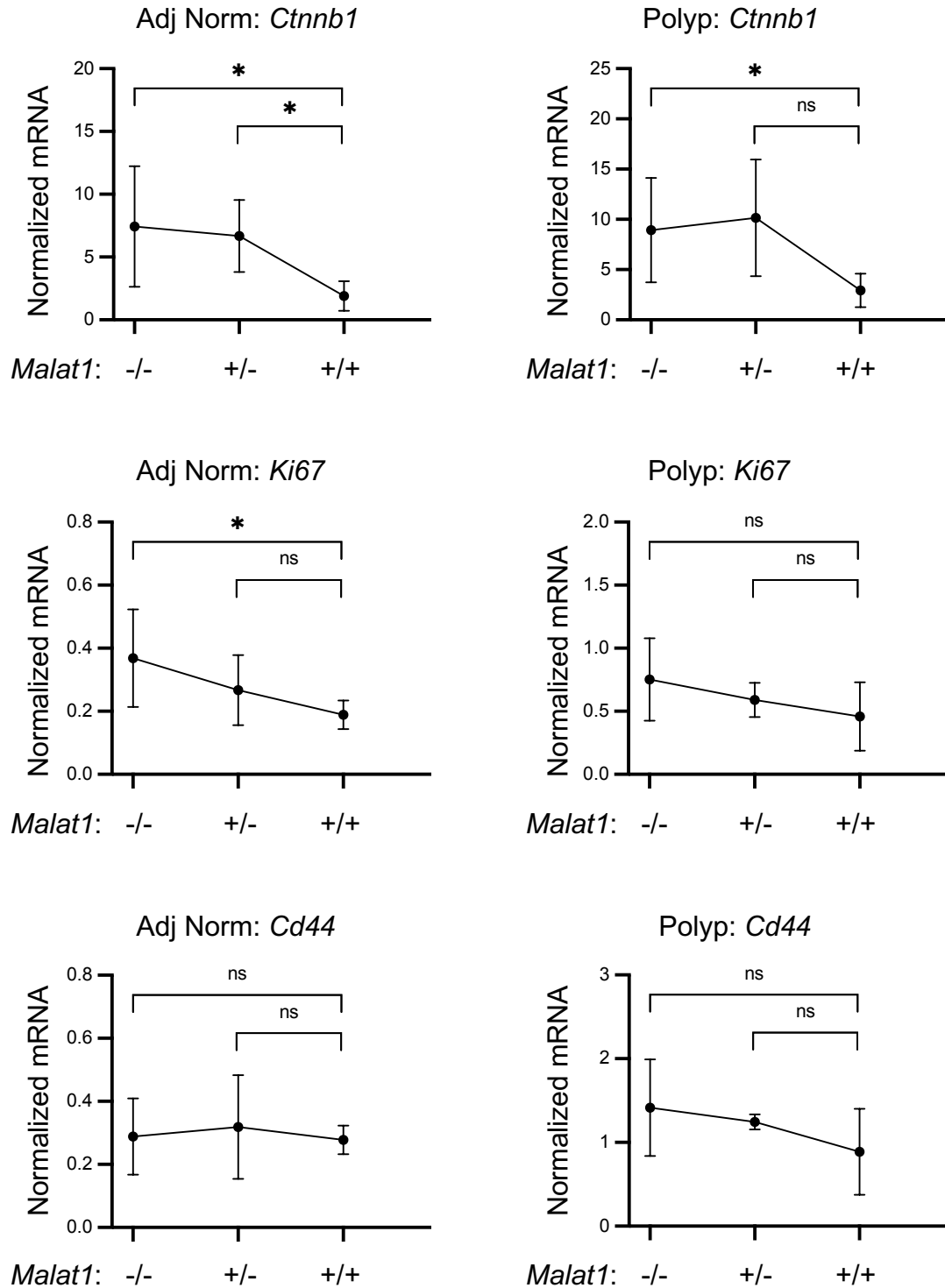


## Colon



Supplementary Fig S3. **Select small intestine gene expression in the polyposis model.**

**A.**



**A.**

